Dynamic Monopoly with Multiple Continuously Distributed Time Delays*

Akio Matsumoto† Ferenc Szidarovszky‡

Abstract

Two time delays are assumed in a boundedly rational monopoly. The characteristic equation is derived for the general case, and a complete stability analysis is conducted both analytically and numerically in two special cases. In the first case in which the continuously distributed time delays have different weights, it is shown that a monopoly equilibrium is destabilized to generate a limit cycle via Hopf bifurcation. In the second case in which one delay is continuously distributed and the other is fixed, it is demonstrated that the stability of the monopoly equilibrium can change finite number of times and eventually becomes periodically or aperiodically unstable. It is of interest to notice that the two delay dynamics can be qualitatively different from the one delay dynamics.

Key words: Boundedly rational, Continuously distributed time delay, Fixed time delay, Hopf bifurcation, Complex dynamics, Gradient dynamics

JEL Classification: C62, C63, D21, D42

*The authors highly appreciate financial supports from the Japan Society for the Promotion of Science (Grant-in-Aid for Scientific Research (C) 24530202) and Chuo University (Grant for Special Research and Joint Research Grant 0981).

†Department of Economics, Chuo University, 742-1, Higashi-Nakano, Hachioji, Tokyo, 192-0393, Japan. akiom@tamacc.chuo-u.ac.jp

‡Department of Systems and Industrial Engineering, University of Arizona, Tucson, 85721-0020, USA. szidar@sie.arizona.edu

1 Introduction

This study analyzes a dynamic model of a boundedly rational monopoly in continuous-time scale and investigates the destabilizing effects caused by time delay arisen in a process of collecting information on the demand function. It is a continuation of Matsumoto and Szidarovszky (2012b) in which the dynamic monopoly model is constructed under a single *continuously distributed time delay* (continuous delay henceforth). The monopoly stationary point is shown to bifurcate to a limit cycle through Hopf bifurcation when it loses stability. It is also a complement of Matsumoto and Szidarovszky (2012a) in which the continuous delay is replaced with a *fixed time delay* (fixed delay henceforth). It is demonstrated that Hopf cycles emerge under one fixed delay and so does the complex dynamics involving chaos under two fixed delays. The point is that periodic behavior emerges if the quantity adjustment process has one time delay, regardless of the delay being continuous or fixed, while aperiodic behavior can be achieved if it contains two fixed delays. The natural inference from these results is that erratic behavior can be expected if multiple continuous delays are involved. The main purpose of this study is to confirm this fact.

The principal impetus is provided by the dynamic analysis of the boundedly rational monopoly with discrete-time scale conducted by Puu (1995) and, more recently, Naimzada and Ricchiuti (2008). A gradient rule is assumed, in both studies, to determine production in such a way that production is increased if a change in profit is positive, decreased if negative and constant if zero. A cubic demand function with an inflection point is assumed in the former and this particular nonlinearity is shown to be a main source for chaotic attractor. On the other hand, a cubic demand without an inflection point is assumed in the latter and stability is violated to chaos through the familiar period-doubling cascade. In this study, the same gradient dynamics is considered under different conditions, namely, the demand function is linear, a continuous-time scale is adopted and the growth rate of output is proportional to the marginal change in expected profit. Special attention is given to the destabilizing effect caused by two continuous delays.

The paper is organized as follows. Section 2 presents a basic monopoly model with continuous delays. Section 3 examines the case in which two continuous delays have different weighting functions. Section 4 investigates the special case in which continuous and fixed delays coexist. Finally concluding remarks are given in Section 5.

2 Delay Monopoly

2.1 Basic Model

Consider an output decision problem of a boundedly rational monopolistic firm which produces output q with marginal cost c. The price function is assumed

to be linear

$$f(q) = a - bq,\ a,\ b > 0.$$

It is further assumed that the firm does not want to react to sudden market changes, so instead of the most current price information, an average of past prices is used in the adjustment process. Because of the linearity of the price function it is equivalent to the use of an average of past output data q^e in the adjustment scheme. Then the corresponding marginal profit is given as $a - c - 2bq^e$ which generates the approximating gradient dynamics

$$\frac{\dot{q}(t)}{q(t)} = \alpha \left(a - c - 2bq^e(t)\right) \tag{1}$$

with $\alpha > 0$ being an adjustment coefficinet, furthermore t denotes a point of continuous time and the dot over a variable means a time derivative. (1) implies that the growth rate of output is adjusted in proportion to the average marginal profit. In constructing best response dynamics, global information is required about the profit function, however, in applying gradient dynamics, only local information is needed. The dynamic equation is written as

$$\dot{q}(t) = \alpha q(t) \left[a - c - 2bq^e(t)\right] \tag{2}$$

Since $q(t) = q^e(t)$ holds at a stationary point, equation (2) has two stationary points; the zero trivial point $q(t) = 0$ and a nontrivial point

$$q^M = \frac{a - c}{2b}$$

where $a > c$ is assumed to ensure that the nontrivial point is positive. We call q^M a *monopoly equilibrium*. Dynamic behavior of (2) depends on the formation of averaging past data. With continuous-time scale, time delays can be modeled with a continuous or fixed delay. As is mentioned in the Introduction, dynamic analysis has been done under the single continuous delay, one and two fixed delays. In this study we adopt multiple continuous delays and draw attention to the destabilizing effects of continuous delays having different weights. In addition we will investigate the limiting case when one delay is continuous and the other is fixed.

2.2 Continuous Delays

In our economic situation with continuous delays, the monopolistic firm gathers information about the actual demands in the past and forms an average by weighting the different transactions according to their likelihood. One particular rule is that weights are exponentially declining with the most weight given to the most current transaction. If the largest weight is given to some past transaction, an appropriate formation rule is that small weight is given to the most current data, rising to maximum at the particular date and declining thereafter. According to the latter rule, weights take a bell-shaped form. We draw attention to the special case in which the firm uses the combination of these different

rules to estimate the incoming demand. To keep the rule simple and tractable, we assume that the firm forms its average with two steps: at the first step the two weighted averages of the past data, $q_1^\varepsilon(t)$ and $q_2^\varepsilon(t)$, are calculated based on the entire history of the same actual output values with different weights; at the second step, the average demand is determined as the weighted average of $q_1^\varepsilon(t)$ and $q_2^\varepsilon(t)$. Since this rule uses the two continuous delays having different weights, we call it the formation rule with *heterogeneous weights* or simply heterogeneous weights.[1] The gradient dynamics with heterogeneous weights is written as the system of the Volterra type integro-differential equations[2]

$$\begin{cases} \dot{q}(t) = \alpha q(t)\left[a - c - 2b\left(\omega q_1^\varepsilon(t) + (1-\omega)q_2^\varepsilon(t)\right)\right], \\ q_1^\varepsilon(t) = \displaystyle\int_0^t W(t-s,S,m)q(s)ds, \\ q_2^\varepsilon(t) = \displaystyle\int_0^t W(t-s,T,n)q(s)ds, \end{cases} \tag{3}$$

where $0 < \omega < 1$, m and n are nonnegative integers, T and S are positive real parameters. The weighting function is defined by

$$W(t-s,\tau,\ell) = \begin{cases} \dfrac{1}{\tau}e^{-\frac{t-s}{\tau}} & \text{if } \ell = 0, \\ \dfrac{1}{\ell!}\left(\dfrac{\ell}{\tau}\right)^{\ell+1}(t-s)^\ell e^{-\frac{\ell(t-s)}{\tau}} & \text{if } \ell \geq 1 \end{cases} \tag{4}$$

for $\tau = S,\ T$ and $\ell = m,\ n$. Parameter τ is associated with the average length of the continuous delay and parameter ℓ determines the shape of the weighting function. For $\ell = 0$, weights are exponentially declining. For $\ell \geq 1$, the shape of the weighting function takes a bell-shaped form which becomes taller and thinner as ℓ increases.

We linearize the dynamic system (3) in a neighborhood of the monopoly equilibrium, to examine local stability. If the actual and average deviations of the output from their equilibrium value at time t are denoted by $q_\delta(t) = q(t) - q^M$

[1] This hybrid rule can arise in a cartel-monopoly situation in which cartel members have different likelihood on the past transactions but agree on a unique pricing.

[2] If the average demand is equal to the fixed delay demand, then the dynamic system can be transformed to a system of delay differential equations, which is rigorously studied in Matsumoto and Szidarovszky (2012b).

and $q^{\varepsilon}_{\delta,i}(t) = q^{\varepsilon}_i(t) - q^M$ for $i = 1, 2$, then linearized version of (3) has the form

$$\begin{cases} \dot{q}_\delta(t) = -\gamma \left[\omega q^{\varepsilon}_{\delta,1}(t) + (1-\omega) q^{\varepsilon}_{\delta,2}(t)\right], \\ q^{\varepsilon}_{\delta,1}(t) = \displaystyle\int_0^t W(t-s,S,m) q_\delta(s) ds, \\ q^{\varepsilon}_{\delta,2}(t) = \displaystyle\int_0^t W(t-s,T,n) q_\delta(s) ds \end{cases} \tag{5}$$

with $\gamma = 2\alpha b q^M$. Substituting the second and third equations of (5) into the first and then substituting the exponential form of the solution, $q_\delta(t) = e^{\lambda t}u$, into the resultant equation present the following form of the characteristic equation

$$\lambda = -\gamma \left[\omega \int_0^t W(t-s,S,m) e^{-\lambda(t-s)} ds + (1-\omega) \int_0^t W(t-s,T,n) e^{-\lambda(t-s)} ds\right].$$

Introducing the new integration variable $t - s = z$ yields

$$\lambda = -\gamma \left[\omega \int_0^t W(z,S,m) e^{-\lambda z} dz + (1-\omega) \int_0^t W(z,T,n) e^{-\lambda z} dz\right].$$

By letting $t \to \infty$, we have

$$\int_0^\infty W(z,\tau,\ell) e^{-\lambda z} dz = \begin{cases} (1+\lambda\tau)^{-1} \text{ if } \ell = 0, \\ \left(1 + \dfrac{\lambda\tau}{\ell}\right)^{-(\ell+1)} \text{ if } \ell \geq 1, \end{cases}$$

with $\tau = S,\ T$ and $\ell = m,\ n$. The usual form of the characteristic equation is therefore

$$\lambda = -\gamma \left[\omega \left(1 + \frac{\lambda S}{\bar{m}}\right)^{-(m+1)} + (1-\omega) \left(1 + \frac{\lambda T}{\bar{n}}\right)^{-(n+1)}\right] \tag{6}$$

where

$$\bar{m} = \begin{cases} 1 \text{ if } m = 0, \\ m \text{ if } m \geq 1, \end{cases} \quad \text{and } \bar{n} = \begin{cases} 1 \text{ if } n = 0, \\ n \text{ if } n \geq 1. \end{cases}$$

Notice that equation (6) can be rewritten as a polynomial equation

$$\lambda \left(1 + \tfrac{\lambda S}{\bar{m}}\right)^{m+1} \left(1 + \tfrac{\lambda T}{\bar{n}}\right)^{n+1} + \gamma \left[\omega \left(1 + \tfrac{\lambda T}{\bar{n}}\right)^{n+1} + (1-\omega) \left(1 + \tfrac{\lambda S}{\bar{m}}\right)^{m+1}\right] = 0 \tag{7}$$

showing that the spectrum is finite with $m + n + 3$ eigenvalues. This is the general form of the characteristic equation with two different continuous delays. It is, however, not easy to derive general stability conditions, so we focus on some special cases with small values of m and n.

Before proceeding, we deal with two cases: the no-delay case as a benchmark and the harmless-delay case. First substituting $S = T = 0$ into equation (7) yields the following form of the characteristic equation,

$$\lambda + \gamma \left[\omega + (1 - \omega)\right] = 0$$

or

$$\lambda = -\gamma = -\alpha(a - c) < 0.$$

The last inequality implies the local asymptotic stability of the monopoly equilibrium since the eigenvalue is real and negative. We next examine the case with $m = n = 0$ in which both delays have exponentially declining weights. The characteristic equation (7) can be written as

$$\lambda(1 + \lambda S)(1 + \lambda T) + \gamma\omega(1 + \lambda T) + \gamma(1 - \omega)(1 + \lambda S) = 0$$

or

$$b_0\lambda^3 + b_1\lambda^2 + b_2\lambda + b_3 = 0 \tag{8}$$

with

$$b_0 = ST,\ b_1 = S + T,\ b_2 = 1 + \gamma\omega T + \gamma(1 - \omega)S \text{ and } b_3 = \gamma.$$

All coefficients are positive. According to the Routh-Hurwitz stability criterion, equation (8) has roots only with negative real parts if and only if

$$b_1 b_2 - b_0 b_3 = (S + T)(1 + \gamma\omega T + \gamma(1 - \omega)S) - ST\gamma > 0$$

where the middle expression is re-written as

$$S^2\gamma(1 - \omega) + T^2\gamma\omega + S + T$$

which is always positive. Hence the monopoly equilibrium is locally asymptotically stable regardless of the values of S and T. In other words, the delays become *harmless* when the weights are exponentially declining. Summarizing these results, we have the following:

Proposition 1 *The monopoly equilibrium is locally asymptotically stable if no delays exist or if the two continuous delays have exponentially declining weighting functions.*

3 Heterogeneous Weights: $m = 0$ and $n \geq 1$

We now examine the case of $m = 0$ and $n \geq 1$ in which delay T has a bell-shaped weight while delay S has a declining weight. Substituting $m = 0$ reduces the characteristic equation (7) to

$$\lambda\left(1 + \lambda S\right)\left(1 + \frac{T}{n}\lambda\right)^{n+1} + \gamma\left[\omega\left(1 + \frac{T}{n}\lambda\right)^{n+1} + (1 - \omega)\left(1 + \lambda S\right)\right] = 0. \tag{9}$$

With expanding the factored terms, this can be reduced to a polynomial equation of degree $n+3$,

$$b_0\lambda^{n+3} + b_1\lambda^{n+2} + \cdots + b_{n+2}\lambda + b_{n+3} = 0 \tag{10}$$

where the coefficients are defined by

$$b_0 = a_0 S,$$

$$b_1 = a_1 S + a_0,$$

$$b_k = a_k S + a_{k-1} + \gamma\omega a_{k-1} \text{ for } 2 \leq k \leq n+1,$$

$$b_{n+2} = a_{n+1} + \gamma\omega a_n + r(1-\omega)S,$$

$$b_{n+3} = \gamma$$

with

$$a_k = \left(\frac{S}{n}\right)^{n+1-k} \begin{pmatrix} m+1 \\ k \end{pmatrix} \text{ for } 0 \leq k \leq n+1.$$

In the case of polynomial equations, the Routh-Hurwitz theorem[3] provides the necessary and sufficient conditions for all the roots to have negative real parts. Applying the theorem, we first construct the $(n+3) \times (n+3)$ Routh-Hurwitz determinant:

$$D_{n+3} = \det \begin{pmatrix} b_1 & b_0 & 0 & 0 & \cdots & 0 \\ b_3 & b_2 & b_1 & b_0 & \cdots & 0 \\ b_5 & b_4 & b_3 & b_2 & \cdots & 0 \\ b_7 & b_6 & b_5 & b_4 & \cdots & 0 \\ \cdot & \cdot & \cdot & \cdot & \cdots & 0 \\ 0 & 0 & 0 & 0 & 0 & b_{n+3} \end{pmatrix}.$$

We then check whether the following two conditions are satisfied:

(S1) all coefficients are positive, $b_k > 0$ for $k = 0, 1, 2, ..., n+3$,

(S2) the principal minors of the Routh-Hurwitz determinant are all positive,

$$D^2_{n+3} > 0,\ D^3_{n+3} > 0, ...\ D^{n+2}_{n+3} > 0$$

where D^k_{n+3} is the k-th order leading principal minor of D_{n+3} and $D^{n+2}_{n+3} > 0$ always leads to $D^{n+3}_{n+3} = \gamma D^{n+2}_{n+3} > 0$ since $\gamma > 0$.

We will investigate local stability in Section 3.1 and then consider global stability in Section 3.2 that is further divided into three parts: the occurrence of Hopf bifurcation is shown in the first part, this analytical result is numerically confirmed in the second part and the destabilizing effect caused by increasing the value of n is examined in the third part.

[3] See, for example, Gandolfo (2009) for this theorem. It is mentioned there that the Liénard-Chipart conditions have an advantage over the Routh-Hurwitze conditions because the former involves about half as many determinantal inequlities as the latter.

3.1 Local Stability

The characteristic equation (10) with $n = 1$ becomes quartic,

$$b_0\lambda^4 + b_1\lambda^3 + b_2\lambda^2 + b_3\lambda + b_4 = 0 \tag{11}$$

with

$$b_0 = ST^2,$$

$$b_1 = 2ST + T^2,$$

$$b_2 = S + 2T + \gamma\omega T^2,$$

$$b_3 = 1 + \gamma(1-\omega)S + 2\gamma\omega T,$$

$$b_4 = \gamma.$$

Since the coefficients are all positive (i.e., condition $(S1)$ is satisfied), the stability condition that all the roots of the characteristic equation have negative real parts is validated if

$$D_4^2 = \det\begin{pmatrix} b_1 & b_0 \\ b_3 & b_2 \end{pmatrix} > 0 \text{ and } D_4^3 = \det\begin{pmatrix} b_1 & b_0 & 0 \\ b_3 & b_2 & b_1 \\ 0 & b_4 & b_3 \end{pmatrix} > 0.$$

Clearly $D_4^3 > 0$ implies $D_4^2 > 0$. Therefore the locus of $D_4^3 = 0$ determines the stability region in case of $n = 1$. In particular, the two loci of $D_4^2 = 0$ and $D_4^3 = 0$ are depicted as C-shaped dotted and solid curves in Figure 1(A) where we take $\gamma = 1$ and $\omega = 1/2$. The inequalities $D_4^3 > 0$ and $D_4^2 > 0$ hold to the left of the corresponding curves and they are reversed to the right. The former curve is located in the region where $D_4^3 < 0$, implying that $D_4^2 > 0$ always in the region where $D_4^3 > 0$. The $D_4^3 = 0$ locus partitions the nonnegative (S, T) plane into a stable (yellow) region and unstable (white) region and thus is called a *partition curve*.

The shape of the $D_4^3 = 0$ locus indicates that equation $D_4^3 = 0$ has equal roots at the turning point of the solid curve. Checking the existence of equal roots, we expand D_4^3 to obtain a quartic polynomial

$$f(T) = aT^4 + bT^3 + cT^2 + dT + d$$

where the coefficients are given by

$$a = 2\omega^2\gamma^2,$$

$$b = 2(1 - 2S\gamma(1-2\omega)),$$

$$c = 2S\gamma(1 - S\gamma\omega),$$

$$d = 4S - (1-\omega)S^2 - (1-\omega)^2\gamma^2S^3,$$

$$e = 2(1 + S\gamma(1-\omega))S^2.$$

It is known that the *resultant* with respect to $f(T)$ and $f'(T)$ is equal to $-\Omega$ where Ω is the discriminant of $f(T)$,

$$\mathrm{Res}(f, f') = \det \begin{pmatrix} a & b & c & d & e & 0 & 0 \\ 0 & a & b & c & d & e & 0 \\ 0 & 0 & a & b & c & d & e \\ 4a & 3b & 2c & d & 0 & 0 & 0 \\ 0 & 4a & 3b & 2c & d & 0 & 0 \\ 0 & 0 & 4a & 3b & 2c & d & 0 \\ 0 & 0 & 0 & 4a & 3b & 2c & d \end{pmatrix} = -\Omega.$$

It is not easy to derive a general form of the equal roots. However, it can be calculated if the parameters are specified. Under the parameter setting ($a = 2$, $b = c = 1$, $\alpha = 1$, $\omega = 1/2$), quartic polynomial $f(T)$ has equal roots at point C with $S_0 \simeq 8.97$ and $T_0 \simeq 4.72$ in Figure 1(A).[4] Then it can be mentioned that the monopoly equilibrium is locally asymptotically stable regardless of the values of T if $S < S_0$. On the other hand, $f(T)$ has two distinct solutions for $S > S_0$. In Figure 1(A), the vertical line at $S = S_1$ crosses the partition curve at two points, A and B, whose coordinates are T_A and T_B, respectively. The monopoly equilibrium loses stability at point A and regains stability at point B when T increases along the vertical line $S = S_1$. Figure 1(B) is the bifurcation diagram with respect to T and depicts that a limit cycle is generated for T in the interval (T_A, T_B) in which the monopoly equilibrium is locally unstable. We will work out the details of this bifurcation diagram and the birth of such cyclic behavior in the next subsection.

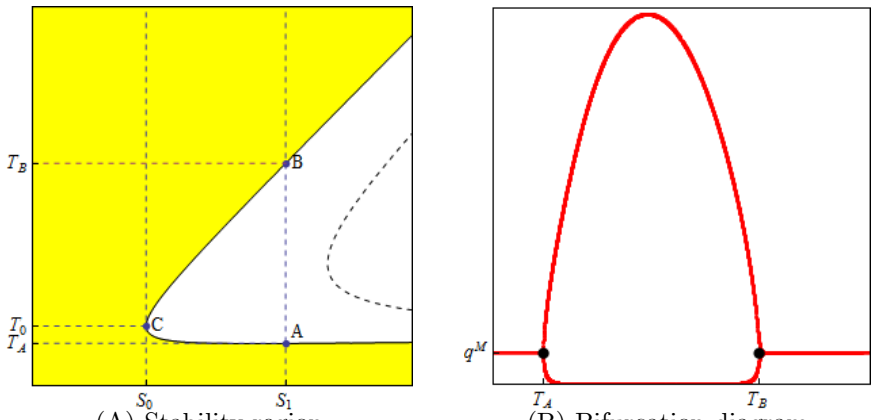

(A) Stability region (B) Bifurcation diagram

Figure 1. Heterogeneous weights with $m = 0$ and $n = 1$

[4] This calculation and the following numerical simulations are done with Mathematica, version 7.

3.2 Global Stability

3.2.1 Hopf Bifurcation

The next question which is naturally arisen is on global dynamics when the equilibrium loses stability. To investigate such dynamics, we will analytically show that a Hopf bifurcation occurs on the partition curve and then numerically confirm the emergence of a limit cycle when the monopoly equilibrium is locally unstable. In order to apply the Hopf bifurcation theorem,[5] we have to check whether the following two conditions are satisfied:

(H1) the characteristic equation has a pair of purely imaginary roots and has no other roots with zero real parts;

(H2) the real part of these roots vary with a bifurcation parameter.

We start with the first condition. The quartic characteristic equation can be factored as follows when $D_4^3 = b_1 b_2 b_3 - b_0^2 b_3 - b_1^2 b_4 = 0$:

$$(b_3 + b_1\lambda^2)(b_1 b_2 - b_0 b_3 + b_1^2\lambda + b_0 b_1 \lambda^2) = 0.$$

It is then clear that the equation has a pair of purely imaginary roots and two roots with no-zero real parts. In particular, the two purely imaginary roots are

$$\lambda_{1,2} = \pm\sqrt{-\frac{b_3}{b_1}} = \pm i\beta$$

with

$$\beta = \sqrt{\frac{1 + \gamma(1-\omega)S + 2\gamma\omega T}{T(2S+T)}}$$

and the other two roots are

$$\lambda_{3,4} = \frac{-b_1^2 \pm \sqrt{b_1^4 - 4b_0 b_1 (b_1 b_2 - b_0 b_3)}}{2b_1 b_2 - b_0 b_3}$$

with

$$\mathrm{Re}\left[\lambda_{3,4}\right] \neq 0.$$

Thus the first condition (H1) is shown to be satisfied.

We turn to verify (H2). Selecting T as a bifurcation parameter, we might treat the characteristic root as a continuous function of T. Then differentiating the characteristic equation (11) with respect to T and arranging terms, we obtain

$$\frac{d\lambda}{dT} = -\frac{ST\lambda^4 + 2T(1+S)\lambda^3 + 2(1+\gamma\omega T)\lambda^2 + 2\gamma(1-\omega)\lambda}{4b_0\lambda^3 + 3b_1\lambda^2 + 2b_1\lambda + b_3}.$$

[5] See, for example, Gandolfo (2009) for this theorem.

At $\lambda = i\beta$, the real part of the derivative is obtained as

$$\mathrm{Re}\left[\frac{d\lambda}{dT}\right] = -\frac{2\beta^2\left\{(ST\beta^2-(1+\gamma\omega T))(b_3-3b_1\beta^2)+2(\gamma\omega-(S+T)\beta^2)(b_2-2b_0\beta^2)\right\}}{(b_3-3b_1\beta^2)^2+4\beta^2(b_2-2b_0\beta^2)^2}. \quad (12)$$

Although the right hand side of (12) has the complicated form, we can numerically check its sign. Given the same setting of the parameters as in Figure 1, the coordinates of points A and B for $S_1 = 20$ are calculated as $T_A \simeq 3.35$ and $T_B \simeq 17.63$, respectively. Substituting these values into the right hand side of equation (12) shows that it is approximately 0.0156 at point A and -0.0015 at point B. Hence we have

$$\mathrm{Re}\left[\left.\frac{d\lambda}{dT}\right|_{\lambda=i\beta}\right] > 0 \text{ at point } A \text{ and } \mathrm{Re}\left[\left.\frac{d\lambda}{dT}\right|_{\lambda=i\beta}\right] < 0 \text{ at point } B.$$

These inequalities imply the fulfillment of the second condition (H2). Hence the equilibrium point loses stability and bifurcates to a limit cycle at point A while the limit cycle merges to the monopoly equilibrium at point B at which stability is regained. It is further possible to demonstrate that the real part of the derivative is positive at any points on the downward-sloping part of the $D_4^3 = 0$ curve and negative on the upward-sloping part in Figure 1(A). The switching of the stability occurs twice when T increases and S is fixed to be larger than S_0.

3.2.2 Numerical Simulations

In this subsection, we numerically examine the stability switch and global behavior of the unstable equilibrium. The dynamic system under the investigation is constructed by substituting $m = 0$ and $n = 1$ into (3),

$$\dot{q}(t) = \alpha q(t)\left[a - c - 2b(\omega q_1^e(t) + (1-\omega)q_2^e(t))\right],$$

$$q_1^e(t) = \int_0^t \frac{1}{S} e^{-\frac{t-s}{S}} q(s)ds,$$

$$q_2^e(t) = \int_0^t \left(\frac{1}{T}\right)^2 (t-s)e^{-\frac{t-s}{T}} q(s)ds.$$

Differentiating the second and third equations with respect to t and introducing a new variable

$$q_0(t) = \int_0^t \frac{1}{T} e^{-\frac{t-s}{T}} q(s)ds$$

reduce the dynamic system with two continuously distributed time delays to a 4D system of the ordinary differential equations,

$$\begin{cases} \dot{q}(t) = \alpha q(t)\left[a - c - 2b(\omega q_1^{\varepsilon}(t) + (1-\omega)q_2^{\varepsilon}(t))\right], \\ \dot{q}_1^{\varepsilon}(t) = \dfrac{1}{S}\left(q(t) - q_1^{\varepsilon}(t)\right), \\ \dot{q}_2^{\varepsilon}(t) = \dfrac{1}{T}\left(q_0(t) - q_2^{\varepsilon}(t)\right), \\ \dot{q}_0(t) = \dfrac{1}{T}\left(q(t) - q_0(t)\right). \end{cases}$$

We use the same parameters setting as before, take initial values, $q(0) = q_1^{\varepsilon}(0) = q_2^{\varepsilon}(0) = q_0(0) = q^M - 0.2$ and then perform simulation of the 4D system for different values of T. Notice that $\gamma = 1$ under this parameter specification. Setting $S_1 = 20$ and increasing the value of T with the increment of 0.01 from 0 to 25 along the vertical line $S = S_1$, we obtain the bifurcation diagram as illustrated in Figure 1(B). For each value of T, the dynamic system is simulated for $10,000$ iterations. The first $9,950$ are discarded and the local minimum and maximum of the remaining 50 data are plotted vertically above the point T. This leaves transient changes out of the picture and gives an estimate of global behavior after initial disturbances. The output trajectory $q(t)$ converges to the monopoly equilibrium for relatively smaller values, $T < T_A$. It loses stability at $T = T_A$ (i.e., point A) and bifurcates to a limit cycle for values up to T_B. The amplitude of the cycle first increases and then decreases as T increases from T_A to T_B. The trajectory regains stability at $T = T_B$ (i.e., point B) and then stays at the equilibrium for $T > T_B$. Essentially the same phenomenon can be observed for any $S > S_0$.

Proposition 2 *Assume heterogeneous weights with $m = 0$ and $n = 1$. Increasing the value of T from zero and fixing $S > S_0$ lead to the followings: (1) two critical values $T_A(S)$ and $T_B(S)$ are obtained by solving $D_4^3 = 0$ for T, given S; (2) a limit cycle is born via Hopf bifurcation when the equilibrium loses stability at $T_A(S)$; (3) the cycle expands, shrinks and then finally merges to the equilibrium point when it regains stability at $T_B(S)$.*

3.2.3 Stability Sensitivity to the Value of n

We have demonstrated that stability of the monopoly equilibrium is sensitive to the length of the delay T, given $S > S_0$. We now draw attention to the value of n to see how the form of the weighting function affects dynamics. As it is clear from (4), the shape of the weighting function depends on the value of the shape parameter n. A larger n means graphically that higher weights are concentrated to a smaller neighborhood of the maximum point $t - T$. The degree of the characteristic equation becomes higher and so does the order of the leading principal minors of the corresponding Routh-Hurwitz determinant.

It then follows that the stability conditions become increasingly untractable. However we can numerically check the stability conditions. Taking the same parameter setting, we illustrate the C-shaped partition curves of $D_{n+3}^{n+2} = 0$ for $n = 1, 2, 3, 4, 5, 6, 7$ in Figure 2(A).[6] The right most curve corresponds to the case of $n = 1$, and the left most curve to $n = 7$, implying that the partition curve shifts leftward as n increases. It is also confirmed that the monopoly equilibrium is locally stable to the left of the corresponding partition curve and unstable to the right. The boundaries of the instability regions are the partition curves painted in black with the interior painted in gray colors. The gray color becomes darker as n increases. Thus the most light-gray region corresponds to the instability region with $n = 1$. The darker gray region surrounded by the right most curve and the next right most curve is added to it to construct the instability region with $n = 2$. The instability regions with $n \geq 3$ are obtained in the same way, implying that the instability region becomes larger as n increases. We present the bifurcation diagrams for $n = 1, 2, 3, 4$ on top of one another in Figure 2(B) where $S = 10$. It can be seen there that an inverse U-shaped part becomes taller and wider with increasing n. This means that the amplitude of the limit cycle becomes larger and the instability interval defined as (T_A^n, T_B^n) becomes longer where T_k^n for $k = A, B$ is a solution of $D_{n+3}^{n+2} = 0$, given $S = 10$.[7] Replacing T for S, n for m and ω for $1 - \omega$, we can derive the partition curves in the case of $n = 0$ and $m \geq 1$. One case with $n \geq 1$ and $m = 0$ can be transformed into the other case with $m \geq 1$ and $n = 0$ by changing variables. This means that the qualitative properties to be obtained do not depend on the choice of fixed and changing variables. So we confine our attention, in the sequel, to the case where m is fixed and n is increased. We have seen the following result:

Proposition 3 *Assume heterogeneous weights with $m = 0$ and $n \geq 1$. Larger values of n have stronger destabilizing effects such that the amplitude of the limit cycle becomes larger and the unstable interval (T_A^n, T_B^n) becomes longer.*

[6] For $n \leq 7$, it is numerically confirmed, as we did in Section 3-1, that $D_{n+3}^{n+2} > 0$ is sufficient to have $D_{n+3}^{k} > 0$ for $k = n + 1, ..., 2$.

[7] Since T_A^n has almost the same values for different value of n, we label only T_A^1 on the horizontal line in Figure 2(B).

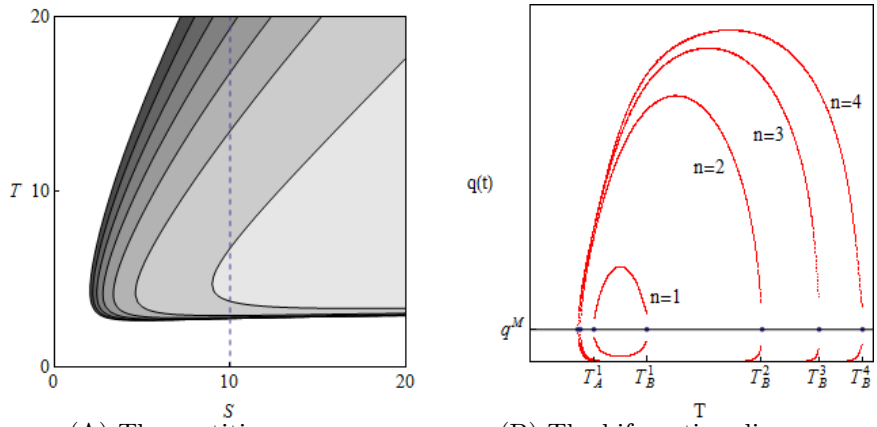

(A) The partition curves (B) The bifurcation diagrams

Figure 2. Heterogeneous weights with $n = 1, 2, ...7$ and $m = 0$.

4 Heterogeneous Delays: $m = 0$ and $n \to \infty$

The expanding instability effect caused by the increasing value of n is numerically confirmed. We now address ourself to an extreme case in which n goes to infinity and m still remains at zero. Since we have

$$\lim_{n\to\infty}\left(1+\frac{\lambda T}{n}\right)^n\left(1+\frac{\lambda T}{n}\right)=e^{\lambda T},$$

the weighting function converges to the Dirac delta function and so does the continuous delay to a fixed delay. The dynamic system (3) turns to be a differential equation with qualitatively different delays, one is a continuous delay and the other is a fixed delay:

$$\begin{cases} \dot{q}(t)=\alpha q(t)\left[a-c-2b(\omega q_1^{\varepsilon}(t)+(1-\omega)q_2^{\varepsilon}(t))\right], \\ q_1^{\varepsilon}(t)=\displaystyle\int_0^t \frac{1}{S}e^{-\frac{t-s}{S}}q(s)ds, \\ q_2^{\varepsilon}(t)=q(t-T). \end{cases}$$

We call this scheme the formation rule with *heterogeneous delays* or simply heterogeneous delays. Substituting the third equation into the first and differentiating the second equation with respect to t, we obtain the following 2D system of a delay differential equation and an ordinary differential equation:

$$\begin{cases} \dot{q}(t)=\alpha q(t)\left[a-c-2b(\omega q_1^{\varepsilon}(t)+(1-\omega)q(t-T))\right] \\ \dot{q}_1^{\varepsilon}(t)=\dfrac{1}{S}\left[q(t)-q_1^{\varepsilon}(t)\right]. \end{cases} \tag{13}$$

Correspondingly the characteristic equation (7) is reduced to

$$\lambda(1+\lambda S)+\gamma\omega+\gamma(1-\omega)(1+\lambda S)e^{-\lambda T}=0 \tag{14}$$

or

$$\lambda^2+a_1\lambda+a_2+(b_1+b_2\lambda)e^{-\lambda T}=0 \tag{15}$$

where the coefficients are

$$a_1=\frac{1}{S},\ a_2=\frac{\gamma\omega}{S},\ b_1=\frac{\gamma(1-\omega)}{S} \text{ and } b_2=\gamma(1-\omega).$$

It has been shown that the monopoly equilibrium is locally stable for $T=0$. We are concerned with whether the stability of the equilibrium switches to instability even under heterogeneous delays when T increases. If such stability switch occurs at $T=\bar{T}$, then the characteristic equation (15) must have a pair of purely imaginary conjugate roots. The central problem of the stability switch is to determine this critical value of $\bar{T}$. To this end, we suppose without loss of generality that $\lambda=i\upsilon,\ \upsilon>0$ is a root of (15) for $T=\bar{T}$ and rewrite the characteristic equation as a set of two equations making the real part and the imaginary part equal to zero,

$$\begin{aligned} &a_2-\upsilon^2+b_1\cos\upsilon T+b_2\upsilon\sin\upsilon T=0,\\ &a_1\upsilon+b_2\upsilon\cos\upsilon T-b_1\sin\upsilon T=0. \end{aligned} \tag{16}$$

Moving $a_2-\upsilon^2$ and $a_1\upsilon$ to the right hand sides of the equations in (16), squaring them and adding them yield

$$b_1^2+b_2^2\upsilon^2=(\upsilon^2-a_2)^2+a_1^2\upsilon^2.$$

Hence

$$\upsilon^4-A\upsilon^2+B=0 \tag{17}$$

where

$$A=b_2^2+2a_2-a_1^2$$

and

$$B=a_2^2-b_1^2=\frac{\gamma^2}{S^2}(2\omega-1).$$

Solving (17) for υ^2 gives two roots

$$\upsilon_{1,2}^2=\frac{A\pm\sqrt{A^2-4B}}{2}.$$

It is proved in the Appendix that the pure imaginary roots of equation (15) are *single*, that is, their multiplicity is one. If $\omega\le 1/2$, then $B\le 0$ leading to $\upsilon_1^2>0$ and $\upsilon_2^2\le 0$. Therefore there is only one nonzero imaginary solution, $\lambda=i\upsilon_1$ with $\upsilon_1>0$. If $\omega>1/2$, then $B>0$ implying the sign-indeterminacy

of $A^2 - 4B$. However, if $A > 0$ and $A^2 > 4B$, then there are two imaginary solutions, $\lambda = i\upsilon_{1,2}$ with $\upsilon_1 > \upsilon_2 > 0$ where

$$\upsilon_1 = \sqrt{\frac{A + \sqrt{A^2 - 4B}}{2}} \text{ and } \upsilon_2 = \sqrt{\frac{A - \sqrt{A^2 - 4B}}{2}}. \tag{18}$$

No imaginary solution exists otherwise, which implies no occurrence of stability switch.

The region classification of the (ω, S) plane is given in Figure 3. There the flat downward-sloping curve is the locus of $A = 0$ below which $A < 0$ and above which $A > 0$. The C-shaped curve is the locus of $A^2 - 4B = 0$, in the left of which $A^2 > 4B$ and in the right of which $A^2 < 4B$.[8] The plane is divided into two subregions by the vertical line $\omega = 1/2$. In the light-gray rectangular to the left of the line, $B < 0$ due to the definition of B. The other subregion on the right is further divided into three parts by the $A = 0$ and $A^2 = 4B$ curves. In the dark-gray region surrounded by the $\omega = 1/2$ line and the upward-sloping part of the $A^2 = 4B$ curve, $A > 0$, $B > 0$ and $A^2 > 4B$. Thus the number of different imaginary roots with positive imaginary parts is zero in the white region, one in the light-gray region and two in the dark-gray region. Our first result in this section concerns dynamics in the white region of Figure 3:

Proposition 4 *Assume heterogeneous delays with $\omega > 1/2$. If $A > 0$ and $A^2 < 4B$ or $A < 0$, then the stability of the monopoly equilibrium does not switch for any $T \geq 0$.*

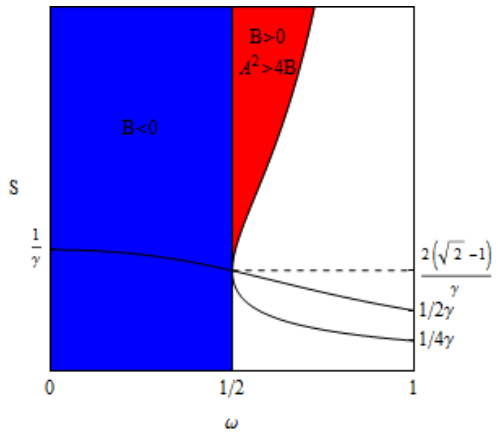

Figure 3. Region classification of the (ω, S) plane

[8] By the coefficient substitutions, we have $A = 0$ as

$$\gamma^2(1-\omega)^2S^2 + 2\gamma\omega S - 1 = 0$$

and $A^2 - 4B = 0$ as

$$\left(\gamma^2(1-\omega)^2S^2 + 1 + 2\gamma\omega S\right)^2 - 4\gamma\omega(1 + 2\gamma\omega S) = 0.$$

In Figure 3, the curves are illustrated under $\gamma = 1$. However this specification does not affect the relative location of the curves.

We verify the emergence of a limit cycle through Hopf bifurcation in the blue and red regions. Selecting T as the bifurcation parameter, we determine the sign of the derivative of $\mathrm{Re}\,\lambda(T)$ at the points where $\lambda(T)$ is purely imaginary. Differentiating implicitly the characteristic equation (15) with respect to T, we obtain

$$\left(\frac{d\lambda}{dT}\right)^{-1} = \frac{(2\lambda + a_1)e^{\lambda T} + b_2}{\lambda(b_2\lambda + b_1)} - \frac{T}{\lambda}.$$

Substituting $\lambda = i\upsilon_{1,2}$ and arranging terms, we can arrive at the following relation

$$sign\left[\left.\frac{d(\mathrm{Re}\,\lambda)}{dT}\right|_{\lambda=i\upsilon_{1,2}}\right] = sign\left[2\upsilon_{1,2}^2 - A\right].$$

Inserting the expressions for υ_1 and υ_2 in (18), it can be seen that the sign is positive for υ_1 and negative for υ_2,

$$sign\left[\left.\frac{d(\mathrm{Re}\,\lambda)}{dT}\right|_{\lambda=i\upsilon_1}\right] = sign\left[\sqrt{A^2 - 4B}\right] \Longrightarrow \left.\frac{d(\mathrm{Re}\,\lambda)}{dT}\right|_{\lambda=i\upsilon_1} > 0 \qquad (19)$$

and

$$sign\left[\left.\frac{d(\mathrm{Re}\,\lambda)}{dT}\right|_{\lambda=i\upsilon_2}\right] = sign\left[-\sqrt{A^2 - 4B}\right] \Longrightarrow \left.\frac{d(\mathrm{Re}\,\lambda)}{dT}\right|_{\lambda=i\upsilon_2} < 0. \qquad (20)$$

Dynamics is qualitatively different according to whether ω is less or greater than $1/2$ or more intuitively whether the parameters are selected from the blue or the red region in Figure 3. We consider the problem of stability switches in the following two cases, $\omega \leq 1/2$ and $\omega > 1/2$.

4.1 Case I: $\omega \leq 1/2$.

In this case, the parameters are selected from the blue region in Figure 3. As is already seen, we have only one imaginary root, $\lambda = i\upsilon_1$ with $\upsilon_1 > 0$. Inequality (19) implies that crossing of the imaginary axis is from left to right as T increases. The stability of the monopoly equilibrium can be lost and not regained. From (16), we have

$$\cos \upsilon_1 T = -\frac{\omega}{(1-\omega)(1+\upsilon_1^2 S^2)} \qquad (21)$$

and

$$\sin \upsilon_1 T = \frac{\upsilon_1(1 - \gamma\omega S + \upsilon_1^2 S^2)}{\gamma(1-\omega)(1+\upsilon_1^2 S^2)}. \qquad (22)$$

There is a unique $\upsilon_1 T$ in the interval $(0, 2\pi]$ such that $\upsilon_1 T$ satisfies both (21) and (22). From (21) the explicit solution of T is given by

$$T_1 = \frac{1}{\upsilon_1}\cos^{-1}\left(-\frac{\omega}{(1-\omega)(1+\upsilon_1^2 S^2)}\right). \qquad (23)$$

Since

$$\begin{aligned} 1-\gamma\omega S+\upsilon_1^2 S^2 &\geq 1-\gamma\omega S+S^2\tfrac{A}{2} \\ &= 1-\gamma\omega S+\tfrac{S^2}{2}\left(\gamma^2(1-\omega)^2+\tfrac{2\gamma\omega}{S}-\tfrac{1}{S^2}\right) \\ &= \tfrac{S^2\gamma^2(1-\omega)^2}{2}>0, \end{aligned}$$

we have $\sin \upsilon_1 T > 0$. This is the smallest stability switch, and at all stability switches the steady state can only lose stability. Notice the following two issues: one is that such a critical value of T is a function of S and the other is that the monopoly equilibrium is asymptotically stable when $0 < T < T_1$ and unstable for $T > T_1$, given S. Their graphical representation with the same parameter setting except $\omega = 2/5$ is given in Figure 4(A) in which the stability region is colored in yellow and its boundary (23) is the partition curve in red. The C-shaped partition curves with $n = 1, 2, ..., 7$ are added in order to compare the stability regions with heterogeneous weights with the one with heterogeneous delays. The vertical dotted line $S = 5$ does not cross the right most C-shaped partition curve, implying that the monopoly equilibrium is always stable if $n = 1$ and $S = 5$. The bifurcation diagram with respect to T along the $S = 5$ line is illustrated in Figure 4(B) where the blue curve is the locus of the maximum and minimum of $q(t)$ under heterogeneous delays and the red curves are the corresponding loci under heterogeneous weights. For graphical simplicity, we label only T_A^2 and T_B^2 on the horizontal axis. Figures 4(A) and 4(B) capture the following three facts. First of all, the C-shaped partition curves tend to the red curve from above as n increases to infinity, implying that the stability region under heterogeneous delays is the smallest. Secondly, due to the different shapes of the partition curves, stability switch occurs only once under heterogeneous delays whereas it occurs twice under heterogeneous weights. And finally, the limit cycle under the heterogeneous delays is larger than the ones under the heterogeneous weights.

Proposition 5 *Assume the heterogeneous delays with $\omega \leq 1/2$. Then there is only one critical value T_1 for each S, and the monopoly equilibrium is asymptotically stable for $T < T_1$ while it becomes locally unstable and bifurcates to a limit cycle for $T > T_1$.*

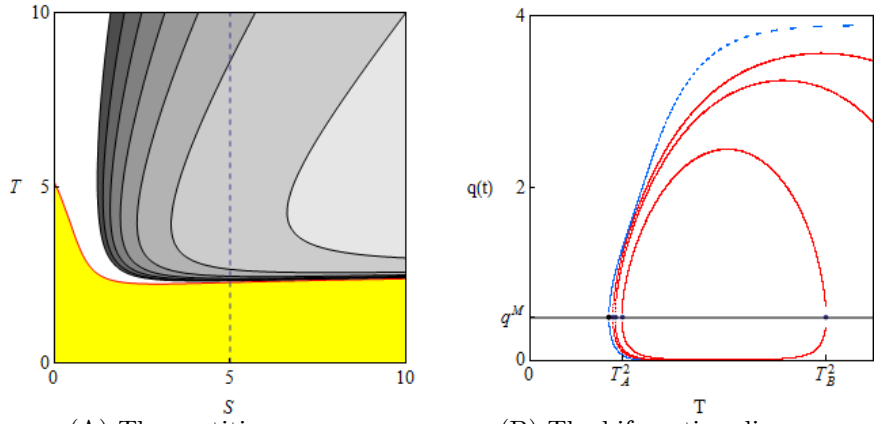

(A) The partition curves (B) The bifurcation diagrams

Figure 4. Heterogeneous weights and delays with $\omega \leq 1/2$

4.2 Case II: $\omega > 1/2$.

In this case, the parameters are selected from the red region of Figure 3. The inequalities in (19) and (20) imply that crossing from left to right with increasing T occurs if $\lambda = i\upsilon_1$ and crossing from right to left occurs if $\lambda = i\upsilon_2$. From equation (16), we obtain the following two sets of the values of T for which there are imaginary roots: for $i = 1, 2$ and $k = 0, 1, 2, ...,$

$$T_{k,i} = \frac{\theta_i}{\upsilon_i} + \frac{2k\pi}{\upsilon_i} \tag{24}$$

where $0 \leq \theta_i = \upsilon_i T_{k,i} < 2\pi$ and

$$\begin{aligned} \cos\theta_i &= -\frac{\omega}{(1-\omega)(1+\upsilon_i^2 S^2)} \\ \sin\theta_i &= \frac{\upsilon_i(1-\gamma\omega S+\upsilon_i^2 S^2)}{\gamma(1-\omega)(1+\upsilon_i^2 S^2)}. \end{aligned} \tag{25}$$

In the red region of Figure 3, we have qualitatively different dynamics from dynamics obtained in the blue region; namely, multiple stability switches under the heterogeneous delays and an emergence of complex dynamics involving chaos. Dynamics is investigated under the same parameter setting except $\omega = 4/5$. We start with the case with $k = 0$. Both $T_{0,1}$ and $T_{0,2}$ obtained from (24) form the partition curve dividing the whole region of (S, T) into stable and unstable regions. In Figure 5(A), the stability region under the heterogeneous delays is colored in yellow and bordered by the red locus of $T_{0,1}$ and the blue locus of $T_{0,2}$ while the partition curves with $n = 2, 3, ..., 7$ under the heterogeneous weights are depicted as black curves as in Figure 2. Given $S = 5$, delays

with $n = 1, 2, 3$ become harmless as the dotted vertical line is located to the left of the partition curve with $n = 3$. In Figure 5(B), the bifurcation diagram under the heterogeneous delays is depicted in blue while those under the heterogeneous weights in red. Seeing Figures 5(A) and 5(B) carefully, we have the following observations. The boundary of the yellow region takes a C-shaped profile which then implies four issues concerning dynamics under the heterogeneous delays: the first is that under the heterogeneous delays T can be harmless when S is less than S_0, the second is that stability switch occurs at least twice when S is larger than S_0, the third is that a limit cycle emerges when the stability is lost, expands, shrinks and then disappears when the stability is regained and the fourth is that the cycle under heterogeneous delays is larger than any cycles under heterogeneous weights.

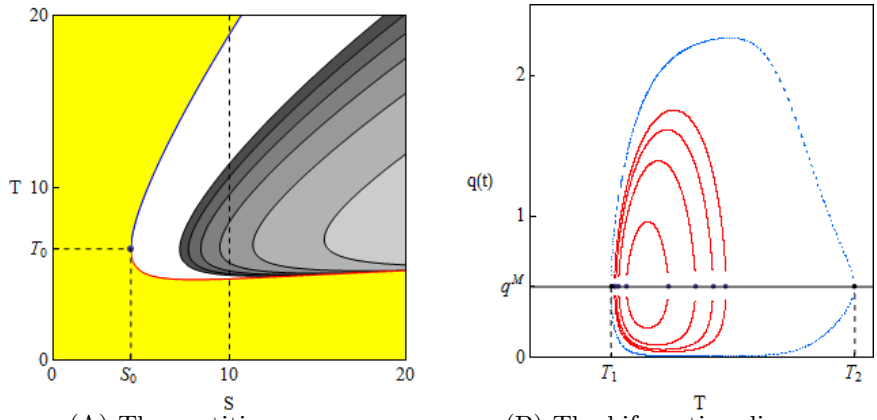

(A) The partition curves (B) The bifurcation diagram

Figure 5. Heterogeneous weights and delays with $\omega > 1/2$

4.3 Finite Number of Stability Switches

Returning to equation (24), we find that the partition curves under heterogeneous delays are also defined for $k \geq 1$. The partition curve for $k = 0$ is constructed by connecting $T_{0,1}$ and $T_{0,2}$. As has been pointed out, its C-shaped profile implies that stability switches occur twice. In the same way the C-shaped partition curve for $k \geq 1$ can be constructed by connecting $T_{k,1}$ and $T_{k,2}$. Therefore there can be a finite number of switches between stability and instability. We present numerical investigations of the multiple stability switches in Figure 6 where the same parameter setting as in Figure 5 is used. The threshold value of S below which the positive delay of T become harmless is obtained as $S_0 \simeq 4.41$. To examine the existence of finite number of stability switches, we select a particular value of S at $S_1 = 5.5 > S_0$ and then perform simulations to see how the dynamics changes when the delay T is increased from zero, fixing $S = S_1$. Figure 6(A) illustrates four partition curves for $k = 0, 1, 2, 3$. Notice that increasing the value of parameter k shifts the corresponding partition

curve vertically upwards. When T is increased along the vertical dotted line at $S = S_1$, the number of roots with $\mathrm{Re}\,\lambda > 0$ is increased by two when T passes through a value of $T_{k,1}$ and it is decreased by two when T passes through a value of $T_{k,2}$ for $k = 0, 1, 2, 3$. These critical values are denoted by the black dots in Figure 6(A) and are in the following order,

$$T_{0,1} < T_{0,2} < T_{1,1} < T_{1,2} < T_{2,1} < T_{3,1} < T_{2,2}.$$

Since $d(\mathrm{Re}\,\lambda)/dT > 0$ at $T = T_{k,1}$ and $d(\mathrm{Re}\,\lambda)/dT < 0$ at $T = T_{k,2}$, two roots have positive real parts for $T > T_{2,1}$ and two additional roots with positive real parts are added when $T > T_{3,1}$. Then only two roots turn to have negative real parts but the other two roots still have positive real parts at $T = T_{2,2}$ at which stability switch from instablity to stablity cannot occur. In consequence, the monopoly equilibrium remains unstable for $T > T_{2,1}$ even though T passes through the critical values of $T_{k,i} > T_{2,1}$. Hence in this example stability switch occurs three times. The equilibrium is locally stable in the three intervals, $[0,\ T_{0,1})$, $(T_{0,2},\ T_{1,1})$ and $(T_{1,2},\ T_{2,1})$ while it is locally unstable in the three intervals $(T_{0,1},\ T_{0,2})$, $(T_{1,1},\ T_{1,2})$ and $(T_{2,1}, \infty]$. In Figure 6(B), we depict a bifurcation diagram with respect to T and observe that the monopoly equilibrium bifurcates to a limit cycle when it loses stability and that the bifurcation scenario is simple in the sense that only limit cycles are repeatedly born finitely many times.

We can also prove analytically that stability switch can occur only finitely many times. Notice that

$$\Delta_{1,k} = T_{k,1} - T_{k-1,1} = \frac{2\pi}{\upsilon_1}$$

and

$$\Delta_{2,k} = T_{k,2} - T_{k-1,2} = \frac{2\pi}{\upsilon_2},$$

and since $\Delta_{1,k} < \Delta_{2,k}$, after finitely many steps a pair $T_{k-1,1}$, $T_{k,1}$ of points will be between two consecutive $T_{k,2}$ values. At this point two pairs of complex roots will have positive real parts and only one of them is able to regain the

negativity of its real part, so the monopoly equilibrium remains unstable.

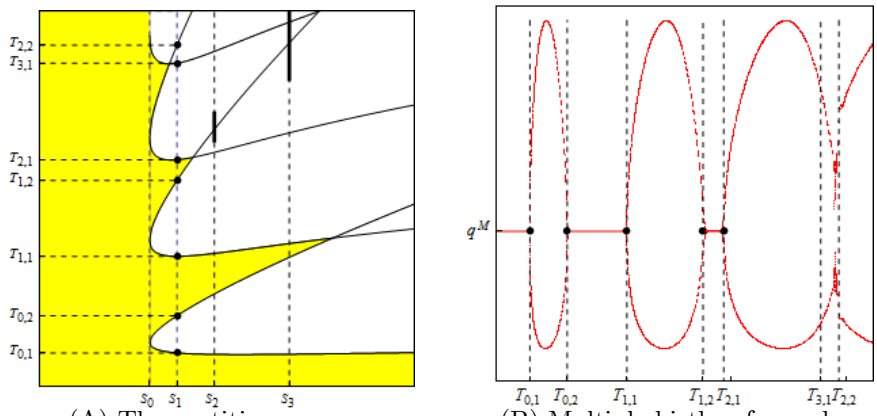

(A) The partition curves (B) Multiple births of a cycle

Figure 6. Several switches between stability and instability for $k = 0, 1, 2, 3$

We perform further simulations to investigate the dynamics for different S-values. The value of S is increased to $S_2 = 7$ from $S_1 = 5.5$. As indicated in Figure 6(A), after losing stability at the second time, the monopoly equilibrium does not regain stability anymore. The bifurcation diagram for $36 < T < 40$ (i.e., the thick part of the vertical line $S = S_2$ in Figure 6(A)) is illustrated in Figure 7(A). It shows that the limit cycle becomes smaller as T increases from 36. The cycle, however, does not merge with the equilibrium point as in Figures 2 but bifurcates to a periodic or aperiodic cycle whose local maximum and minimum points correspond to the plotted points spread over some region of the output $q(t)$. The value of S is further increased to $S_3 = 10$ and then the delay dynamic system (13) is numerically simulated again along the thick part of the vertical line $S = S_3$. The resultant dynamics is summarized in Figures 7(B) where complex dynamics is born. The bifurcation diagram illustrates the following result. The limit cycle turns to be a period-2 cycle which has two local maxima and two local minima. Around $T = 48$, two extrema suddenly appear and then the limit cycles bifurcate to complex dynamics. The bifurcation scenario is different from the well-known period-doubling route to chaos and the one given in Figure 7(A). We can now summarize the dynamic results under heterogeneous delays:

Proposition 6 *Assume heterogeneous delays with $\omega > 1/2$. If $A > 0$ and $A^2 > 4B$, then (i) there are two imaginary roots with positive real parts, and the stability of the monopoly equilibrium can change a finite number of times and (ii) the unstable equilibrium bifurcates to a limit cycle or aperiodic oscillations as T increases when S is small or large.*

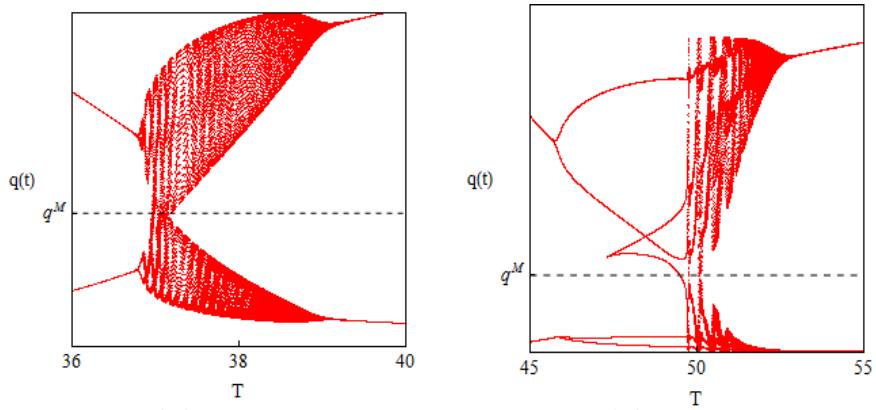

(A) $S = 7$ (B) $S = 10$

Figure 7. Bifurcation diagrams

5 Concluding Remarks

We have analytically and numerically examined dynamics of a boundedly rational monopoly with two continuous delays. The general form of the characteristic equation was derived and then attention was focused on two special cases. In the first case in which two continuous delays have different weights, we show that a monopoly equilibrium is destabilized and a limit cycle is born through Hopf bifurcation with increasing length of the delay. We also show that the limit cycle expands, shrinks and then finally merges to the monopoly equilibrium with further increase. In the second case in which one delay is continuous and the other is fixed, we demonstrate the following result, in addition to the delay effects obtained in the first case: stability and instability of the monopoly equilibrium are alternating finitely many times and afterwords, the equilibrium becomes unstable. Lastly it is numerically confirmed that aperiodic dynamics can be emerged for large values of the delays.

It is of interest to note that this study expands our earlier result in Matsumoto and Szidarovszky (2012b) where monopoly dynamics under one continuous delay can generate only simple dynamics such as limit cycles. Our analysis implies that the presence of multiple continuous delays can result in complex dynamics involving chaos.

Appendix

In this appendix we show that eigenvalues $\lambda = i\upsilon$ of equation (15) are *single*. For convenience, we write equation (15) as

$$\lambda^2 + a_1\lambda + a_2 + (b_1 + b_2\lambda)e^{-\lambda T} = 0. \tag{A-1}$$

If a root $\lambda = i\upsilon$ is multiple, then

$$2\lambda + a_1 + b_2 e^{-\lambda T} + (b_1 + b_2\lambda)e^{-\lambda T}(-T) = 0. \tag{A-2}$$

From (A-1),

$$e^{-\lambda T} = -\frac{\lambda^2 + a_1\lambda + a_2}{b_1 + b_2\lambda}$$

and from (A-2)

$$2\lambda + a_1 + (b_2 - Tb_1 - Tb_2\lambda)\left(-\frac{\lambda^2 + a_1\lambda + a_2}{b_1 + b_2\lambda}\right) = 0.$$

It can be rewritten as

$$Tb_2\lambda^3 + (b_2 + Tb_1 + Ta_1b_2)\,\lambda^2 + (2b_1 + Ta_1b_1 + Ta_2b_2)\lambda + (a_1b_1 - a_2b_2 + Ta_2b_1) = 0$$

where coefficients are

$$Tb_2 = \gamma(1-\omega)T,$$

$$b_2 + Tb_1 + Ta_1b_2 = \gamma(1-\omega)\left(1 + \tfrac{2T}{S}\right),$$

$$2b_1 + Ta_1b_1 + Ta_2b_2 = \gamma(1-\omega)\left(\tfrac{2}{S} + \tfrac{T}{S^2} + \tfrac{T\gamma\omega}{S}\right),$$

$$a_1b_1 - a_2b_2 + Ta_2b_1 = \gamma(1-\omega)\left(\tfrac{1}{S^2} - \tfrac{\gamma\omega}{S} + \tfrac{T\gamma\omega}{S^2}\right).$$

Simplifying with $\gamma(1-\omega)$ in all coefficients reduces the last equation to

$$T\lambda^3 + \left(1 + \frac{2T}{S}\right)\lambda^2 + \left(\frac{2S + T + ST\gamma\omega}{S^2}\right)\lambda + \frac{1 - S\gamma\omega + T\gamma\omega}{S^2} = 0.$$

If $\lambda = i\upsilon$, then real and imaginary parts give

$$\upsilon^2 = \frac{1 - S\gamma\omega + T\gamma\omega}{S^2 + 2TS}$$

and

$$\upsilon^2 = \frac{2S + T + ST\gamma\omega}{TS^2}$$

implying that

$$\frac{1 - S\gamma\omega + T\gamma\omega}{S^2 + 2TS} = \frac{2S + T + ST\gamma\omega}{TS^2}$$

or

$$2S^2\,(1 + T\gamma\omega) + T\,(4S + 2T + TS\gamma\omega) = 0$$

which is impossible. Therefore all pure imaginary roots are single.

References

[1] Bellman, R. and K. L. Cooke, *Differential-difference Equations,* Academic Press, New York, 1956.

[2] Bischi, G-I, C. Chiarella, M. Kopel and F. Szidarovszky, *Nonlinear Oligopolies: Stability and Bifurcations*, Springer-Verlag, Berlin/Heidelberg/New York, 2010.

[3] Cushing, J., *Integro-differential Equations and Delay Models in Population Dynamics*, Springer-Verlag, Berlin/Heidelberg/New York, 1977.

[4] Gandolfo, G., *Economic Dynamics*, *4th Edition*, Springer-Verlag, Berlin/Heidelberg/New York, 2009.

[5] Matsumoto, A. and F. Szidarovszky, "Nonlinear Delay Monopoly with Bounded Rationality," *Chaos, Solitions and Fractals*, vol. 45, 507-519, 2012a.

[6] Matsumoto, A. and F. Szidarovszky, "Boundedly Rational Monopoly with Continuously Distributed Single Time Delay," *InER Discussion Paper #180*, Institute of Economic Research (InER), Chuo University (http://www2.chuo-u.ac.jp/keizaiken/discuss.htm), 2012b.

[7] Naimzada, A. and G. Ricchiuti, "Complex Dynamics in a Monopoly with a Rule of Thumb," *Applied Mathematics and Computation*, vol. 203, 921-925, 2008.

[8] Okuguchi, K. and F. Szidarovszky, *The Theory of Oligopoly with Multi-Product Firms*, Springer-Verlag, Berlin/Heidelberg/New York, 1990.

[9] Puu, T., "The Chaotic Monopolist," *Chaos, Solitons and Fractals*, vol. 5, 34-44, 1995.